

1 Inter-annual variations of wet deposition in Beijing during 2014-2017:
2 implications of below-cloud scavenging of inorganic aerosols

3
4 Baozhu Ge^{1,5*}, Danhui Xu¹, Oliver Wild², Xuefeng Yao³, Junhua Wang^{1,4}, Xuechun
5 Chen¹, Qixin Tan^{1,4}, Xiaole Pan¹, Zifa Wang^{1,4,5*}

6 ¹ State Key Laboratory of Atmospheric Boundary Layer Physics and Atmospheric
7 Chemistry (LAPC), Institute of Atmospheric Physics (IAP), Chinese Academy of
8 Sciences (CAS), Beijing 100029, China

9 ² Lancaster Environment Centre, Lancaster University, LA1 4YQ, United Kingdom

10 ³ PLA 96941 Army, Beijing 102206, China

11 ⁴ University of Chinese Academy of Sciences, Beijing, 100049, China

12 ⁵ Center for Excellence in Regional Atmospheric Environment, Institute of Urban
13 Environment, Chinese Academy of Sciences, Xiamen 361021, China

14 *Correspondence to: Baozhu Ge (gebz@mail.iap.ac.cn) and Zifa Wang
15 (zifawang@mail.iap.ac.cn)

16 **Abstract**

17 Wet scavenging is an efficient pathway for the removal of particulate matter (PM) from
18 the atmosphere. High levels of PM have been a major cause of air pollution in Beijing
19 but have decreased sharply under the Air Pollution Prevention and Control Action Plan
20 launched in 2013. In this study, four years of observations of wet deposition have been
21 conducted using a sequential sampling technique to investigate the detailed variation in
22 chemical components through each rainfall event. We find that the major ions, SO_4^{2-} ,
23 Ca^{2+} , NO_3^- and NH_4^+ , show significant decreases over the 2013-2017 period (decreasing
24 by 39%, 35%, 12% and 25%, respectively), revealing the impacts of the Action Plan.
25 An improved method of estimating the below-cloud scavenging proportion based on
26 sequential sampling is developed and implemented to estimate the contribution of
27 below-cloud and in-cloud wet deposition over the four-year period. Overall, the below-
28 cloud scavenging plays a dominant role to the wet deposition of four major ions at the
29 beginning of the Action Plan. The contribution of below-cloud scavenging for Ca^{2+} ,
30 SO_4^{2-} and NH_4^+ decreases from above 50% in 2014 to below 40% in 2017. This suggests
31 that the Action Plan has mitigated PM pollution in the surface layer and hence decreased
32 scavenging due to the washout process. In contrast, we find little change in the annual
33 volume weighted average concentration for NO_3^- where the contribution from below-
34 cloud scavenging remains at ~44% over the period 2015-2017. While highlighting the
35 importance of different wet scavenging processes, this paper presents a unique new
36 perspective on the effects of the Action Plan and clearly identifies oxidized nitrogen
37 species as a major target for future air pollution controls.

38 **Key words:** wet scavenging, below-cloud, in-cloud, deposition, $\text{PM}_{2.5}$

40 **1 Introduction**

41 Atmospheric wet deposition is a key removal pathway for air pollutants and is governed
42 by two main processes: in-cloud and below-cloud scavenging (Goncalves et al., 2002;
43 Andronache, 2003, 2004a; Henzing et al., 2006; Sportisse, 2007; Feng, 2009; Wang et
44 al., 2010; Zhang et al., 2013). The below-cloud scavenging process depends both on
45 the characteristics of the rain (snow), including the raindrop size distribution and
46 rainfall rate, and on the chemical nature of the particles and their concentration in the
47 atmosphere (Chate et al., 2003). Previously, below-cloud scavenging was thought to be
48 less important than in-cloud processes and was simplified or even ignored in many
49 global and regional chemical transport models (CTMs) (Barth et al., 2000; Tang et al.,
50 2005; ENVIRON.Inc, 2005; Textor et al., 2006; Bae et al., 2010). However, more recent
51 extensive research on wet scavenging has found that precipitation, even light rain, can
52 remove 50-80% of the number or mass concentration of below-cloud aerosols, and this
53 is supported by both field measurements and semi-empirical parameterizations of
54 below-cloud scavenging in models (Andronache, 2004b; Zhang et al., 2004; Wang et al.,
55 2014). Xu et al. (2017;2019) studied the below-cloud scavenging mechanism based on
56 the simultaneous measurement of aerosol components in rainfall and in the air in
57 Beijing. They found that below-cloud scavenging coefficients for $PM_{2.5}$ widely used in
58 CTMs ($\sim 10^{-5}$ - 10^{-6}) were 1-2 orders of magnitude lower than estimates from
59 observations (at the range of 10^{-4} - 10^{-5} for SO_4^{2-} , NO_3^- and NH_4^+ , respectively). This
60 implies that the simulated below-cloud scavenging of aerosols might be significantly
61 underestimated. This could be one reason for the underestimation of SO_4^{2-} and NO_3^-
62 wet deposition in regional models of Asia reported in phase II and III of the Model
63 Inter-Comparison Study for Asia (MICS-Asia) (Wang et al., 2008; Itahashi et al., 2020;
64 Ge et al., 2020) and in global model assessments by the Task Force on Hemispheric
65 Transport of Atmospheric Pollutants (TF-HTAP) (Vet et al., 2014), in addition to the
66 other sources of model uncertainties (Chen et al., 2019; Tan et al., 2020; Kong et al.,
67 2020), such as emissions, chemical transformation and changes in other ambient
68 compounds of sulfur and nitrogen. Bae et al. (2012) added a new below-cloud
69 scavenging parameterization scheme in the CMAQ model and improved the simulation

70 of aerosol wet deposition fluxes in East Asia by as much as a factor of two compared
71 with observations. The below-cloud scavenging process is critical not only for wet
72 deposition but also for the concentration of aerosols in the air and it should be
73 represented appropriately in CTM simulations.

74 It is important to recognize the contribution of below-cloud scavenging to total wet
75 deposition. However, many studies have found that it is difficult to separate the two wet
76 scavenging processes based on measurement methods alone (Huang et al., 1995; Wang
77 and Wang, 1996; Goncalves et al., 2002; Bertrand et al., 2008; Xu et al., 2017). A
78 commonly used approach to separating below-cloud scavenging from total wet
79 deposition is through sequential sampling (Aikawa et al., 2014; Ge et al., 2016; Aikawa
80 and Hiraki, 2009; Wang et al., 2009; [Quyang et al., 2015](#); Xu et al., 2017). In this way,
81 precipitation composition during different stages of a rainfall event can be investigated
82 separately in the lab after sampling. The chemical components in later increments of
83 rainfall are thought to be less influenced by the below-cloud scavenging process than
84 by the in-cloud [scavenging](#) process (Aikawa et al., 2014; 2009). Xu et al. (2017) applied
85 this approach to summer rainfall in Beijing in 2014 and found that more than 50% of
86 deposited sulfate, nitrate and ammonium ions were from below-cloud scavenging. In
87 this study, an innovated method based on exponential curve to chemical ions in rainfall
88 by sequential sampling is developed and implemented to estimate the ratio of below-
89 cloud to in-cloud wet deposition in Beijing over the four-year period between 2014 and
90 2017. Together with PM_{2.5} concentration measurements, the [below-cloud scavenging](#)
91 effects of the decreasing air pollutants at near-surface due to the Air Pollution
92 Prevention and Control Action Plan (Action Plan) launched in 2013 (State Council of
93 the People's Republic of China, 2019) is also investigated to explore the implications
94 of the Action Plain to the precipitation chemistry.

95 **2 Data and methods**

96 **2.1 Measurement site and sampling methodology**

97 The measurement site is located on the roof of a two-floor building at the Institute of
98 Atmospheric Physics tower site (IAP-tower, 39° 58' 28" N, 116° 22' 1" E) in northern
99 Beijing. It is a typical urban site between the 3rd and 4th ring roads and lying close to

100 the Badaling expressway (Xu et al., 2017;2019;Sun et al., 2015). Four years of Inter-
101 annual observations of each rainfall event were conducted at this site. Sequential
102 sampling of each rainfall event is employed to catch the evolution of precipitation
103 composition during each event. To investigate the detailed variation in the concentration
104 of different chemical components in precipitation, especially the sharp changes
105 occurring during the onset of rainfall, high resolution sampling of rainfall at 1 mm
106 sequential increments was performed using an automatic wet-dry sampler. The
107 rainwater collector uses a circular polyethylene board with a 30 cm diameter and
108 collects up to eight fractions. About 70 ml of rainwater is collected for each of the first
109 seven fractions and the rest of the rainfall is collected in the eighth fraction. For example,
110 if there is 12 mm rainfall volume in a precipitation event, 1 mm sequential rainfall is
111 collected in each of the first 7 fractions with the rest of 5 mm in the eighth fraction.
112 Rainfall events where eight fractions are collected and identified as full events, and
113 those with fewer than eight fractions are characterized as incomplete events. Manual
114 sampling methods were used to collect more than eight fractions during heavy rainfall,
115 and these are characterized as extended events. During 2014-2017, a total of 104
116 precipitation events, which is almost 690 precipitation samples, were collected. Of the
117 total number of precipitation events, 33 events (32%) were discarded from the
118 sequential sampling analysis due to low rainfall amounts (<8 mm), which cannot satisfy
119 the rules of full events. Altogether, 69 full events including 6 extended events were
120 recorded over the 2014-2017 period in Beijing, as 15, 16, 20 and 18 events at each year,
121 respectively. The rainfall volume of the eighth fraction of these 69 full events varied
122 from 1 mm to 55.9 mm.

123 After collection, all samples are refrigerated at 0-4 °C and analyzed at the Key
124 Laboratory for Atmospheric Chemistry, Chinese Academy of Meteorological Sciences
125 (CAMS) within one month, following the procedure used for the Acid Rain Monitoring
126 Network run by the China Meteorological Administration (CMA-ARMN) (Tang et al.,
127 2007;2010). Nine ions that include four anions (SO_4^{2-} , NO_3^- , Cl^- and F^-) and five cations
128 (NH_4^+ , Na^+ , K^+ , Ca^{2+} and Mg^{2+}) are detected using ion chromatography (IC, Dionex
129 600, USA). Their relative standard deviations in reproducibility tests are less than 5%.

130 Quality assurance is carried out using routine standard procedure of blind sample inter-
131 comparison organized by CMA (Tang et al., 2010). Quality control is conducted by
132 assessment of the anion-cation balance and by comparison of the calculated and
133 measured conductivity. A more detailed description of the procedure can be found in
134 Ge et al. (2016) and Xu et al. (2017).

135 **2.2 Aerosol measurements**

136 Aerosol mass concentration is recorded in routine measurements for the observation
137 network of the China National Environmental Monitoring Center (CNEMC). PM_{2.5}
138 concentrations are used from the Olympic Park station, a monitoring station located 3
139 km to the northeast of the IAP-tower sampling site. In addition, an Ambient Ion
140 Monitor-Ion Chromatograph (AIM-IC) developed by URG Corp., Chapel Hill, NC and
141 Dionex Inc., Sunnyvale, CA, is used to measure PM_{2.5} composition at the sampling site
142 between 2014 and 2017. This instrument includes a sample collection unit (URG 9000-
143 D) for collection of water-soluble gases and particles in aqueous solution and a sample
144 analysis unit (two ion chromatographs, Dionex ICS-2000 and ICS-5000) for analysis
145 of both anions and cations. The limit of detection of AIM-IC is 0.08 mg/m³ for NH⁴⁺
146 and 0.1 mg/m³ for the other ions. Aerosol mass concentrations and composition are both
147 measured at 1 h time resolution. Detailed descriptions of the AIM-IC instrumentation
148 can be found in Malagutti et al. (2015) and Markovic et al. (2012). The average
149 concentration of aerosols in the 6 h before each rainfall event is calculated to reflect the
150 air pollution conditions before the event. For comparisons, the yearly average
151 concentration of aerosols has been calculated to represent the normal conditions.

152 **2.3 Estimation of below cloud scavenging**

153 Previous studies have shown that the concentration of chemical ions in precipitation
154 decreases through the progression of a rainfall event and eventually stabilizes at low
155 levels (Aikawa and Hiraki, 2009;2014;Ge et al., 2016;Xu et al., 2017). The **in-cloud**
156 and **below-cloud scavenging** contributions to total wet deposition are estimated based
157 on the assumption that the concentrations in later increments can be attributed to
158 scavenging by rainout only. This assumption relies on the efficient scavenging of air
159 pollutants below cloud through the evolution of precipitation. However, the

concentration of chemical ions in precipitation may also be affected by many other factors in addition to below-cloud air pollutant concentrations and in-cloud scavenging processes. For example, the precipitation intensity may affect the scavenging efficiency of air pollutants below cloud and hence influence wet deposition (Andronache, 2004b; Wang et al., 2014; Xu et al., 2017; 2019). Yuan et al. (2014) reported that in central North China high intensity rainfall events of short duration (lasting less than 6 h) are dominant rather than long-duration rainfall that is more common in the Yangtze River Valley. Therefore, the time window for the definition of in cloud stage is very important for estimating the below cloud and in cloud contributions. Previous studies have estimated the concentration of chemical ions scavenged in-cloud based on the judgment that 5 mm of accumulated precipitation is sufficient to identify the contribution of the in-cloud scavenging process (Wang et al., 2009; Aikawa and Hiraki, 2009; Xu et al., 2017). Based on this approach, the concentration of NO_3^- and SO_4^{2-} in cloud in Japan was found to be 0.70 and 1.30 mg/L, respectively (Aikawa and Hiraki, 2009). In Beijing, high concentration of NH_4^+ , SO_4^{2-} and NO_3^- during 2007 were found at 2.1~5.5, 3.1~14.9, 1.5~5.9 mg/L, respectively (Wang et al., 2009; Xu et al., 2017).

In this study, a new method based on fitting a curve to the chemical ion concentrations with successive rainfall increments has been developed to estimate the contribution of the in-cloud process. As shown in Figure 1, an exponential curve is fitted to the median, 25th and 75th percentiles of the chemical ion concentrations in each fraction through the rainfall increments. Noted that, the fitted exponential curve is applied to the combination of all 69 full events to estimate the yearly median concentration of chemical ions in-cloud and to compare with the results from previously reported method (i.e., median concentration after 5 mm increments). Besides, the exponential approach to each unique event was also employed. Ideally, the concentration of chemical ions stabilize at higher rainfall increments and this represents the concentration in cloud. However, the decrease during each rainfall event is distinctly different, and this regression method is not fully applicable to all rainfall events in practice. Therefore, the exponential regression method is used to estimate the in-cloud concentration under most circumstances, but where the decreasing trend with the

190 increment of rainfall is not significant, the average value of rainfall increments 6-8 of
191 the event is used. The below cloud contributions to wet deposition of each species are
192 then calculated using the following equations (1-2):

193
$$\text{Wetdep}_{\text{below-cloud}} = \sum_{i=1}^n (C_i - \bar{C}) \times P_i \quad (1)$$

194
$$\text{Contribution}_{\text{below-cloud}} = \frac{\text{Wetdep}_{\text{below-cloud}}}{\sum_{i=1}^n C_i \times P_i} \quad (2)$$

195 Where, C_i , and \bar{C} represent the concentration of each chemical ion in fraction i and in
196 cloud and P_i represents the volume of rainfall, while n represent the total fractions in
197 a rainfall event (equally to 8 in this study).

198 **3 Results and Discussion**

199 **3.1 Inter-annual variations in chemical components**

200 The Action Plan is launched in 2013 called “Ten rules” to improve the air quality in
201 China. It includes comprehensive control of industrial emission, non-point emission,
202 fugitive dust, vehicles, etc. It is also aimed to adjust and optimize the industrial
203 structure and promote economic transformation and upgrading, such as increase the
204 supply of clean energy. These actions are ensured to work by both of legislation and
205 market mechanism. According to the *Beijing Environmental Statement* published by the
206 Beijing Municipal Environmental Protection Bureau from 2013 to 2017, many
207 measures have been implemented to meet the Action Plan, including replacement
208 residential coal with electricity and natural gas, upgrading the emission standards of
209 gasoline, diesel vehicles and power plants, closing the high-emission enterprises.

210 Significant declines in atmospheric PM_{2.5} concentration have been observed nationwide
211 between 2013 and 2017 during the Action Plan (Zhang et al., 2019). However, few
212 studies have investigated the benefits of the Action Plan for wet deposition. A decrease
213 in the ratio of SO₄²⁻/NO₃⁻ mostly due to the decreasing of SO₄²⁻ and increasing of NO₃⁻
214 suggests the transformation of sulfuric acid type to a mixed type of sulfuric and nitric
215 acid in North China. However, the updated record especially after the Action Plan is
216 important to assess the mitigation of the air pollutants not only in the atmosphere but
217

also in rainfall. A nationwide investigation of the wet deposition of inorganic ions in 320 cities across China was recently made based on observations between 2011 and 2016 from the National Acid Deposition Monitoring Network (NADMN), which was established by the China Meteorological Administration (Li et al., 2019). Briefly, both SO_4^{2-} and NO_3^- across China experienced significant changes before and after 2014, with increases from 2011 to 2014 and then decreases from 2014 to 2016. In order to quantify the influence of the Action Plan on wet deposition in Beijing, four years of observations of each rainfall event are considered in this study. Figure 2 shows the volume weighted average (VWA) of inter-annual mean concentrations of SO_4^{2-} , NO_3^- , NH_4^+ and Ca^{2+} observed in Beijing during 2014 to 2017 along with those reported before 2010 from previous studies (Yang et al., 2012; Pan et al., 2012, 2013) (more detail is provided in Table S1 in supplementary materials). A continuous decrease in VWA concentrations between 1995 and 2017 is found for SO_4^{2-} and Ca^{2+} , with decreases of $3.1\% \text{ yr}^{-1}$ and $36.1\% \text{ yr}^{-1}$ in the earlier stage (1995-2010) and decreases of $9.8\% \text{ yr}^{-1}$ and $8.8\% \text{ yr}^{-1}$ in the later stage (2014-2017). This is consistent with the annual changes in its emission and concentration as shown in Figure 3, in which the emission and the concentration data are collected from the yearly book of "*Environmental Bulletin in Beijing*" from 1994 to 2017. It is clearly shown the concentration of SO_2 experienced a sustainably decreasing trend due to significant reduction of its emission from 1996 to 2017, with the decreases rate is $4.5\% \text{ yr}^{-1}$ and $13.9\% \text{ yr}^{-1}$ in emission and $2.8\% \text{ yr}^{-1}$ and $14.0\% \text{ yr}^{-1}$ in concentration during earlier stage and the later stage (the Action Plan period), respectively. For NO_3^- and NH_4^+ , increases are found during the earlier stage ($\sim 60\%$) and decreases in the later stage (12% for NO_3^- and 25% for NH_4^+). As to NO_x emission, the data in recent years have been collected. Although the clearly reduction is found in the annual changes of emission from 2010, the ambient concentration of NO_2 do not show a significant decreasing trend ($\sim 3.6\% \text{ yr}^{-1}$) compared with SO_2 ($14\% \text{ yr}^{-1}$). However, before the Action Plan, the decreasing ratio in concentration is only $1.8\% \text{ yr}^{-1}$, which is slower than the Action Plan period. Despite the increases of VWA NO_3^- in precipitation during the earlier stage, the small decreases in later stage would also be attributed to the Action Plan. All four components in the

249 later stage show significant decreases, suggesting that the Action Plan, which was
250 implemented over this period, has a substantial impact. While Ca^{2+} and SO_4^{2-} played a
251 prominent role in precipitation during the earlier stage before 2010, NH_4^+ and NO_3^-
252 became the primary components in the later stage after 2010. It should be noted that
253 NH_4^+ has a double role in environment pollution because it mitigates acid rain through
254 neutralization, but also acidifies the soil by nitrification. Hence, while sulfur in
255 precipitation has been further reduced under the Action Plan, additional attention is
256 needed for nitrogen to prevent deterioration of the environment by acid rain resulting
257 from nitrate and ammonium.

258 **3.2 Relationship in concentrations in precipitation and the atmosphere**

259 Wet deposition of a substance involves its removal from the associated air mass. The
260 scavenging ratio H can be estimated by comparing the monthly average concentration
261 in precipitation with that in the air (Okita et al., 1996;Kasper-Giebl et al., 1999;Hicks,
262 2005;Yamagata et al., 2009). Xu et al. (Xu et al., 2017) first calculated the rainfall event
263 H based on the hourly concentration of aerosol components measured with an Aerodyne
264 Aerosol Chemical Speciation Monitor (ACSM) and AIM-IC in 2014. In this study four
265 years of observation of aerosol components have been undertaken by AIM-IC.
266 Measurements made in the 6 hours before each rainfall event are averaged to represent
267 the precondition of wet deposition precursors in the atmosphere. Figure 4 shows the
268 relationship between the major chemical ions in precipitation and in the air. The VWA
269 concentration of SO_4^{2-} , NO_3^- and NH_4^+ (hereafter SNA) as well as Ca^{2+} in each rainfall
270 event has been calculated and compared with that in the first 1 mm rainfall fraction,
271 F1#. As shown in Figure 4, positive correlations are found between the concentrations
272 of ions in precipitation and in air, with Pearson correlation coefficients (R) generally
273 higher than 0.7 ($p<0.01$). The concentration in the first fraction should represent a high
274 proportion of below-cloud scavenging due to the washout of air pollutants below clouds
275 by the first rainfall, while the VWA represents a greater contribution from in-cloud
276 removal (Aikawa and Hiraki, 2009;Wang et al., 2009;Xu et al., 2017). Thus, it is
277 reasonable that the correlations are stronger for the first fraction than for the VWA, see
278 Table 1. This indicates that the concentration of chemical ions in precipitation at the

279 start of rainfall is more greatly influenced by the air pollutants below the cloud. As
280 rainfall continues and below-cloud concentrations are reduced, there is an increased
281 contribution from in-cloud scavenging, which is less influenced by aerosols in the
282 surface layer. This is confirmed by the substantial difference in the two R coefficients
283 for the cation ion Ca^{2+} (0.85 for the first fraction, 0.47 for the VWA), which often exists
284 in coarse particles below cloud. For the fine particle SO_4^{2-} which is present both in and
285 below clouds (Xu et al., 2017), the difference in the two R coefficients is small. The R
286 coefficients for NO_3^- and NH_4^+ show less difference than Ca^{2+} , but larger difference
287 than SO_4^{2-} . This may relate to their complicate sources from the ambient precursors.
288 For example, the NO_3^- in precipitation is both from the fine and coarse particles (i.e.,
289 particulate NO_3^-) as well as the gaseous HNO_3 , while the NH_4^+ in precipitation is mainly
290 from the fine particles in addition to NH_3 .

291 The slope of the linear fits in Figure 4 can be used to calculate the scavenging ratio
292 W , which is the ratio of the ions concentration in precipitation (mg/L) and in air ($\mu\text{g}/\text{m}^3$).
293 The W ratio is 0.25×10^6 , 0.16×10^6 and 0.15×10^6 for SNA, SO_4^{2-} , NO_3^- and NH_4^+
294 respectively. This is similar to that reported for rainfall events in 2014 in Beijing
295 (0.26×10^6 , 0.35×10^6 and 0.14×10^6 for SNA) by Xu et al. (2017) and consistent with
296 those estimated in the eastern United States (0.11 - 0.38×10^6 , 0.38 - 0.97×10^6 and 0.2 -
297 0.75×10^6 for SNA) (Hicks, 2005). Compared with SO_4^{2-} and NH_4^+ , the scavenging ratio
298 for NO_3^- shows larger differences between this study and previous studies,
299 corresponding to larger uncertainties to the R between the concentrations of ions in
300 precipitation and in air for VWA in Figure 4a (lower significance $p < 0.05$). It should be
301 noted that the W calculated in this study is based on the fine particles in air, which
302 may not represent the accurate reflection of the wet scavenging efficiency of SNA.

303 Wet deposition can affect much of the atmospheric column through in-cloud and
304 below-cloud scavenging processes. The vertical column density (VCD) of SO_2 and NO_2
305 from satellite during 2000s to 2017 is used here to compare with the inter-annual
306 variations in wet deposition in Beijing (Figure S1). Consistent variation of the VCD
307 and the yearly VWA concentration in precipitation is found in S and N. A continuous
308 decrease is found in VCD SO_2 from 2005 to 2017, matching the trend in SO_4^{2-}

309 deposition, while for VCD NO₂ shows an increase from 2001 to 2011, a decrease after
310 2011 and little change over the [period](#) 2014-2017. This implies that the Action Plan not
311 only benefits air pollutants in the surface layer but also those in the total column. Due
312 to faster decreases in emissions of S than N (Zheng et al., 2018), the ratio of S/N in both
313 precipitation (SO₄²⁻/NO₃⁻, $\mu\text{eq/L}$) and air (SO₄²⁻/NO₃⁻, $\mu\text{g/m}^3$) are found to decrease,
314 with the change in ratio in precipitation at 17.5% yr^{-1} , 11% yr^{-1} and 20.0 % yr^{-1} during
315 1995-2010, 2014-2017 and 1995-2017, and in air at 12% yr^{-1} during 2014-2017,
316 respectively, see Figure S2. [This is also consistent with the trend reported in whole](#)
317 [China during 2000-2015 by Itahashi et al. \(2018\)](#). The ratio of S/N in precipitation is a
318 [useful index to investigate the relative contributions of these acidifying species](#). In
319 addition, the ratio of NH₄⁺/NO₃⁻ is investigated here and a clear decrease is found during
320 2014-2017 both in precipitation and in air. This indicates that NH₄⁺ is decreasing faster
321 than NO₃⁻. This evidence clearly confirms that nitrate should be the major target for air
322 pollution controls in the next Action Plan.

323 **3.3 Proportion of below cloud scavenging**

324 As described in section 2.3, the in-cloud ion concentration (\bar{C} , in Eq 1) can be derived
325 from the exponential fit of the observed rainwater concentrations. Table 2 lists the
326 asymptote value and the exponential fitting equation of the evolution of each ion
327 concentration in precipitation with the increment of rainfall. As shown, the asymptote
328 value (here after, exponential approach) based on the median data for SO₄²⁻, NO₃⁻ and
329 NH₄⁺ was 3.18 mg/L, 2.32 mg/L and 1.39 mg/L, respectively. The SO₄²⁻ and NO₃⁻ are
330 within the range of reported in cloud concentrations for Beijing (3.33 mg/L and 2.75
331 mg/L for SO₄²⁻ and NO₃⁻ in Xu et al., 2017), while the NH₄⁺ in this study is lower than
332 previous studies (2.51 mg/L in Xu et al., 2017 and 2.1-4.5 mg/L in Wang et al., 2009).
333 In-cloud concentrations for other ions, i.e., Ca²⁺, F⁻, Cl⁻, Na⁺, K⁺ and Mg²⁺, are 0.67
334 mg/L, 0.04 mg/L, 0.27 mg/L, 0.1 mg/L, 0.06 mg/L and 0.08 mg/L, respectively. For
335 comparison, the average concentration in fractions 6 to 8 (F6#~F8#) in each rainfall
336 event (here after, average approach) is used to estimate the in-cloud concentration for
337 events where successive rainwater concentrations do not show an obvious decrease or
338 where other factors such as precipitation intensity are important, see Table 2. Similar

339 results are found for most ions with the exponential and average approach except for
340 NH_4^+ , F^- , K^+ and Mg^{2+} , where the maximum difference is less than 20% (Table 2). Thus,
341 the replacement of in-cloud concentration by the average value is acceptable for SO_4^{2-} ,
342 NO_3^- , Ca^{2+} , Cl^- and Na^+ but much uncertainty for the other ions. It is worth noting that
343 for all ions the average approach gives higher estimates of in-cloud concentrations, and
344 this can be recognized as an upper limit for in-cloud concentrations.

345 Following Eq (2), the contribution of below-cloud scavenging to wet deposition in
346 each rainfall event during 2014-2017 are estimated from the in-cloud concentration.
347 Figure 5 shows the yearly VWA of SNA and Ca^{2+} and the in-cloud and below-cloud
348 contributions. The ratio of below-cloud contribution to the four major components
349 based on the yearly median value of the in-cloud concentration is also shown in Figure
350 5. Benefiting from the Action Plan, the air quality at the surface layer have been
351 significantly improved (Zhang et al., 2019), which in turn leading to the decreases of
352 the below-cloud scavenging. In this study, it also shows the below-cloud contributions
353 of SO_4^{2-} , NO_3^- , NH_4^+ and Ca^{2+} decreases from >50% in 2014 to ~40% in 2017. In 2017,
354 the contribution of below-cloud scavenging declines to lower than 40% for SO_4^{2-} and
355 NH_4^+ , but remains at 44% for NO_3^- . Over the four-year period 2014-2017, the average
356 yearly wet deposition for all ions and the below-cloud wet scavenging contributions are
357 given in Table 2. Similar to the concentrations in precipitation, the wet deposition of
358 SO_4^{2-} , NO_3^- , NH_4^+ decreased from $21.5 \text{ kgS ha}^{-1} \text{ yr}^{-1}$, 8.9 and $19.0 \text{ kg N ha}^{-1} \text{ yr}^{-1}$ during
359 2007-2010 (Pan et al., 2012; 2013) to $11.4 \text{ kgS ha}^{-1} \text{ yr}^{-1}$ ($3.42 \times 10^3 \text{ mg m}^{-2} \text{ yr}^{-1}$), 6.9 and
360 $16.7 \text{ kgN ha}^{-1} \text{ yr}^{-1}$ (3.05×10^3 and $2.15 \times 10^3 \text{ mg m}^{-2} \text{ yr}^{-1}$) during 2014-2017, respectively.
361 Below-cloud scavenging contributed to almost half of total deposition estimated with
362 the exponential approach (50~60%), higher than the average approach (40~50%).

363 **4 Factors influencing below-cloud scavenging**

364 **4.1 Rainfall type**

365 The rainfall over the North China Plain in summer time is usually determined by the
366 synoptic system such as the upper-level trough or the cold vortex. The 75 rainfall events
367 have been classified based on synoptic system according to records from the Beijing
368 Meteorological Service (<http://bj.cma.gov.cn>) with 33 events associated with upper-

369 level troughs, 23 events associated with a cold vortex and 19 events associated with
370 other systems. Figure 6 shows the contributions of below-cloud scavenging for the two
371 major systems. A high contribution from below-cloud scavenging is found for rainfall
372 events associated with an upper-level trough with the median contributions for SO_4^{2-} ,
373 NO_3^- , NH_4^+ and Ca^{2+} of 56.2%, 62.1%, 56.3% and 61.9%, respectively. In the contrast,
374 the contributions during rainfall events under cold vortex conditions are significant
375 lower, with the values of 42.2%, 44.5%, 41.7% and 53.9%, respectively. Rainfall events
376 associated with an upper-level trough are usually accompanied by orographic or frontal
377 precipitation and are characterized by long and continuous precipitation (Shou et al.,
378 2000). This suggests that below-cloud scavenging of chemical components is important
379 for this rainfall type due to air mass transport from outside Beijing. In contrast, rainfall
380 events associated with a cold vortex usually originate from strong thermal convection
381 and are characterized by short heavy rainfall (Zhang et al., 2008; Liu et al., 2016; Zheng
382 et al., 2020). This is common during the summer months in Beijing with deep
383 convective clouds (Yu et al., 2011; Gao and He, 2013), and suggests that there is a large
384 contribution from in-cloud scavenging to the total wet deposition.

385 **4.2 Precipitation intensity and rainfall volume**

386 To illustrate the impacts of rainfall on below-cloud aerosol scavenging, the relationship
387 between the below-cloud fraction and the rainfall volume and precipitation intensity are
388 investigated, see Figure 7. Negative correlations in below cloud fraction are found for
389 both the rainfall volume and precipitation intensity, although the relationship with the
390 former is stronger ($R: 0.63\sim0.93$ vs. $0.03\sim0.64$). This is consistent with results for 2014
391 in Beijing reported by Xu et al. (2017). Atmospheric particles are efficiently removed
392 below cloud by washout at the beginning of precipitation events (almost 70% of SNA
393 is removed in the first 2-3 fractions, as shown in Figure 1). As the rainfall progresses,
394 in-cloud **scavenging** makes an increasingly important contribution as below-cloud
395 aerosol concentrations fall. Xu et al. (2017) found that heavy summertime rainfall
396 events with more than 40 mm of rainfall usually occur over very short periods of time,
397 usually 2-3 h. This heavy rainfall leads to the scavenging of aerosols in a relatively
398 localized region and prevents the compensation associated with transport of air

399 pollutants from outside the region during longer-duration light rainfall events. This
400 contributes to the decreased contribution of below-cloud scavenging during the high
401 intensity rainfall events.

402 **5 Conclusions**

403 This paper presents an analysis of below-cloud scavenging from four years of
404 sequential sampling of rainfall events in Beijing from May of 2014 to November of
405 2017. The concentration of ions in precipitation varied dramatically, with yearly volume
406 weighted averaged concentrations of SO_4^{2-} , NO_3^- , NH_4^+ and Ca^{2+} decreasing by 39%,
407 12%, 25% and 35% between 2014 and 2017, respectively. Due to faster decreases in
408 SO_4^{2-} than NO_3^- both in precipitation and in the air during the observation period, there
409 is a significant decrease in S/N ratio in precipitation at 44% and in air at 48%.
410 Benefiting from the national Air Pollution Prevention and Control Action Plan, the
411 sulfur has been further reduced, while the nitrogen, especially nitrate, needs further
412 attention in the next Action Plan to prevent deterioration of the environment associated
413 with acid rain and photochemical pollution.

414 A new method has been developed and employed to estimate the below-cloud
415 contribution to wet deposition in Beijing. The new approach suggests that the
416 contribution from below-cloud scavenging is greater than that estimated applying
417 simpler approaches used in previous studies. [Overall, the contribution of below-cloud](#)
418 [scavenging to the wet deposition of the four major components is important at 50~60%.](#)
419 The contribution of below-cloud scavenging shows a decrease over the period 2014-
420 2017 for Ca^{2+} , SO_4^{2-} and NH_4^+ , but little change for NO_3^- during 2015-2017. Below-
421 cloud scavenging also has a strong cleansing effect on air pollution, and the hourly
422 concentration of $\text{PM}_{2.5}$ is found to decrease sharply as the rainfall events occur, even
423 with the effects from wind swept out have been accounted for.

424 Rainfall types also influence the contribution of below-cloud scavenging. Seventy-
425 five rainfall events during the four-year periods were classified based on the local
426 synoptic conditions. Lower contributions from below-cloud scavenging (~40%) are
427 found for the four major ions in rainfall events associated with a cold vortex, while
428 higher contributions (~60%) occurred associated with an upper-level trough.

429 Precipitation volume and intensity both show a negative correlation with the below-
430 cloud fraction. This suggests that atmospheric particles are efficiently removed via
431 **below-cloud scavenging** processes at the beginning of precipitation events. As the event
432 progresses, rainfall in the later fractions shows a greater contribution from in-cloud
433 **scavenging** processes as aerosols in the surface layer have already been **removed**. To
434 better understand the mechanism of **below-cloud scavenging** processes, high resolution
435 of measurement both in precipitation and in the air especially at the beginning of rainfall
436 events are needed in the future.

437

438 **Data availability.**

439 To request observed data for scientific research purposes, please contact Baozhu Ge at
440 the Institute of Atmospheric Physics, Chinese Academy of Sciences, via email
441 (gebz@mail.iap.ac.cn).

442

443 **Author contribution**

444 BG and ZW designed the whole structure of this work, and prepared the manuscript
445 with contributions from all co-authors. DX, XY, JW and QT helped with the data
446 processing. OW, XC and XP was involved in the scientific interpretation and discussion.

447

448 **Competing interests**

449 The authors declare that they have no conflict of interest

450

451 **Acknowledgment**

452 We appreciate CNEMC for providing the data of the 6 criteria pollutants in Beijing. We
453 also appreciate Beijing Municipal Environmental Monitoring Center for providing the
454 aerosol components data in Beijing. This work is supported by the National Natural
455 Science Foundation of China (Grant No 41877313, 91744206, 41620104008), Priority
456 Research Program (XDA19040204) and the Key Deployment Program (ZDRW-CN-
457 2018-1-03) of the Chinese Academy of Sciences.

458

459 **References:**

460 Aikawa, M., and Hiraki, T.: Washout/rainout contribution in wet deposition estimated
461 by 0.5 mm precipitation sampling/analysis, *Atmos Environ*, 43, 4935-4939, 2009.

462 Aikawa, M., Kajino, M., Hiraki, T., and Mukai, H.: The contribution of site to washout
463 and rainout: Precipitation chemistry based on sample analysis from 0.5 mm
464 precipitation increments and numerical simulation, *Atmos Environ*, 95, 165-174,
465 <http://dx.doi.org/10.1016/j.atmosenv.2014.06.015>, 2014.

466 Andronache, C.: Estimated variability of below-cloud aerosol removal by rainfall for
467 observed aerosol size distributions, *Atmospheric Chemistry and Physics*, 3, 131-
468 143, 2003.

469 Andronache, C.: Estimates of sulfate aerosol wet scavenging coefficient for locations
470 in the Eastern United States, *Atmospheric Environment*, 38, 795-804,
471 [10.1016/j.atmosenv.2003.10.035](http://dx.doi.org/10.1016/j.atmosenv.2003.10.035), 2004a.

472 Andronache, C.: Precipitation removal of ultrafine aerosol particles from the
473 atmospheric boundary layer, *J Geophys Res-Atmos*, 109, 2004b.

474 Bae, S. Y., Jung, C. H., and Kim, Y. P.: Derivation and verification of an aerosol
475 dynamics expression for the below-cloud scavenging process using the moment
476 method, *J Aerosol Sci*, 41, 266-280, 2010.

477 Bae, S. Y., Park, R. J., Yong, P. K., and Woo, J. H.: Effects of below-cloud scavenging
478 on the regional aerosol budget in East Asia, *Atmos Environ*, 58, p.14-22, 2012.

479 Barth, M. C., Rasch, P. J., Kiehl, J. T., Benkovitz, C. M., and Schwartz, S. E.: Sulfur
480 chemistry in the National Center for Atmospheric Research Community Climate
481 Model: Description, evaluation, features, and sensitivity to aqueous chemistry, *J*
482 *Geophys Res-Atmos*, 105, 1387-1415, 2000.

483 Bertrand, G., Celle-Jeanton, H., Laj, P., Rangognio, J., and Chazot, G.: Rainfall
484 chemistry: long range transport versus below cloud scavenging. A two-year study
485 at an inland station (Opme, France), *J Atmos Chem*, 60, 253-271, 2008.

486 Chate, D. M., Rao, P. S. P., Naik, M. S., Momin, G. A., Safai, P. D., and Ali, K.:
487 Scavenging of aerosols and their chemical species by rain, *Atmospheric
488 Environment*, 37, 2477-2484, [10.1016/S1352-2310\(03\)00162-6](http://dx.doi.org/10.1016/S1352-2310(03)00162-6), 2003.

489 Chen, L., Gao, Y., Zhang, M., Fu, J. S., Zhu, J., Liao, H., Li, J., Huang, K., Ge, B.,
490 Wang, X., Lam, Y. F., Lin, C. Y., Itahashi, S., Nagashima, T., Kajino, M., Yamaji,
491 K., Wang, Z., and Kurokawa, J.: MICS-Asia III: multi-model comparison and
492 evaluation of aerosol over East Asia, *Atmos. Chem. Phys.*, 19, 11911-11937,

493 Feng, J.: A size - resolved model for below - cloud scavenging of aerosols by snowfall,
494 *Journal of Geophysical Research*, 114, [10.1029/2008jd011012](http://dx.doi.org/10.1029/2008jd011012), 2009.

495 Gao, Y., and He, L. F.: The phase features of a cold vortex over north China (in English
496 abstract), *J Appl Meteor Sci*, 24, 704-713, 2013.

497 Ge, B., Wang, Z., Gbaguidi, A. E., and Zhang, Q.: Source Identification of Acid Rain
498 Arising over Northeast China: Observed Evidence and Model Simulation, *Aerosol
499 Air Qual Res*, 16, 1366-1377, [10.4209/aaqr.2015.05.0294](http://dx.doi.org/10.4209/aaqr.2015.05.0294), 2016.

500 Ge, B., Itahashi, S., Sato, K., Xu, D., Wang, J., Fan, F., Tan, Q., Fu, J. S., Wang, X.,
501 Yamaji, K., Nagashima, T., Li, J., Kajino, M., Liao, H., Zhang, M., Wang, Z., Li,

502 M., Woo, J. H., Kurokawa, J., Pan, Y., Wu, Q., Liu, X., and Wang, Z.: MICS-Asia
503 III: Multi-model comparison of reactive Nitrogen deposition over China, *Atmos.*
504 *Chem. Phys. Discuss.*, 2020, 1-43, 10.5194/acp-2019-1083, 2020.

505 Goncalves, F. L. T., Ramos, A. M., Freitas, S., Dias, M. A. S., and Massambani, O.: In-
506 cloud and below-cloud numerical simulation of scavenging processes at Serra Do
507 Mar region, SE Brazil, *Atmos Environ.*, 36, 5245-5255, 2002.

508 Gryspeerd, E., Stier, P., White, B. A., and Kipling, Z.: Wet scavenging limits the
509 detection of aerosol effects on precipitation, *Atmos. Chem. Phys.*, 15, 7557-7570,
510 10.5194/acp-15-7557-2015, 2015.

511 Henzing, J. S., Olivie, D. J. L., and van Velthoven, P. F. J.: A parameterization of size
512 resolved below cloud scavenging of aerosols by rain, *Atmospheric Chemistry and*
513 *Physics*, 6, 3363-3375, 2006.

514 Hicks, B. B.: A climatology of wet deposition scavenging ratios for the United States,
515 *Atmos Environ.*, 39, 1585-1596, 2005.

516 Huang, M., Shen, Z., and Liu, S.: A study on the formation processes of acid rain in
517 some areas of Southwest China (in Chinese), *Scientia Atmopherica Sinica*, 19, 359-
518 366, 1995.

519 Itahashi, S., Yumimoto, K., Uno, I., Hayami, H., Fujita, S. I., Pan, Y., and Wang, Y.: A
520 15-year record (2001–2015) of the ratio of nitrate to non-sea-salt sulfate in
521 precipitation over East Asia, *Atmos. Chem. Phys.*, 18, 2835-2852, 10.5194/acp-18-
522 2835-2018, 2018.

523 Itahashi, S., Ge, B., Sato, K., Fu, J. S., Wang, X., Yamaji, K., Nagashima, T., Li, J.,
524 Kajino, M., Liao, H., Zhang, M., Wang, Z., Li, M., Kurokawa, J., Carmichael, G.
525 R., and Wang, Z.: MICS-Asia III: overview of model intercomparison and
526 evaluation of acid deposition over Asia, *Atmos. Chem. Phys.*, 20, 2667-2693,
527 10.5194/acp-20-2667-2020, 2020.

528 Kasper-Giebl, A., Kalina, M. F., and Puxbaum, H.: Scavenging ratios for sulfate,
529 ammonium and nitrate determined at Mt. Sonnblick (3106 m asl), *Atmos Environ.*,
530 33, 895-906, 1999.

531 Kong, L., Tang, X., Zhu, J., Wang, Z., Fu, J. S., Wang, X., Itahashi, S., Yamaji, K.,
532 Nagashima, T., Lee, H. J., Kim, C. H., Lin, C. Y., Chen, L., Zhang, M., Tao, Z., Li,
533 J., Kajino, M., Liao, H., Wang, Z., Sudo, K., Wang, Y., Pan, Y., Tang, G., Li, M.,
534 Wu, Q., Ge, B., and Carmichael, G. R.: Evaluation and uncertainty investigation of
535 the NO₂, CO and NH₃ modeling over China under the framework of MICS-
536 Asia III, *Atmos. Chem. Phys.*, 20, 181-202, 10.5194/acp-20-181-2020, 2020.

537 Li, R., Cui, L., Zhao, Y., Zhang, Z., Sun, T., Li, J., Zhou, W., Meng, Y., Huang, K., and
538 Fu, H.: Wet deposition of inorganic ions in 320 cities across China: spatio-temporal
539 variation, source apportionment, and dominant factors, *Atmos. Chem. Phys.*, 19,
540 11043-11070, 10.5194/acp-19-11043-2019, 2019.

541 Liu, X. M., Zhang, M. J., Wang, S. J., Zhao, P. P., Wang, J., and Zhou, P. P.: Estimation
542 and analysis of precipitation cloud base height in China (in english abstract),
543 *Meteor Mon.*, 42, 1135-1145, 2016.

544 Malaguti, A., Mircea, M., La Torretta, T. M. G., Telloli, C., Petralia, E., Stracquadanio,
545 M., and Berico, M.: Comparison of Online and Offline Methods for Measuring

546 Fine Secondary Inorganic Ions and Carbonaceous Aerosols in the Central
547 Mediterranean Area, *Aerosol Air Qual Res*, 15, 2641-2653, 2015.

548 Markovic, M. Z., VandenBoer, T. C., and Murphy, J. G.: Characterization and
549 optimization of an online system for the simultaneous measurement of atmospheric
550 water-soluble constituents in the gas and particle phases, *J Environ Monitor*, 14,
551 1872-1884, 2012.

552 Okita, T., Hara, H., and Fukuzaki, N.: Measurements of atmospheric SO₂ and SO₄²⁻,
553 and determination of the wet scavenging coefficient of sulfate aerosols for the
554 winter monsoon season over the Sea of Japan, *Atmos Environ*, 30, 3733-3739,
555 1996.

556 Ouyang, W., Guo, B. B., Cai, G. Q., Li, Q., Han, S., Liu, B., and Liu, X. G.: The washing
557 effect of precipitation on particulate matter and the pollution dynamics of rainwater
558 in downtown Beijing, *Sci Total Environ*, 505, 306-314, 2015.

559 Pan, Y. P., Wang, Y. S., Tang, G. Q., and Wu, D.: Wet and dry deposition of atmospheric
560 nitrogen at ten sites in Northern China, *Atmos Chem Phys*, 12, 6515-6535, 2012.

561 Pan, Y. P., Wang, Y. S., Tang, G. Q., and Wu, D.: Spatial distribution and temporal
562 variations of atmospheric sulfur deposition in Northern China: insights into the
563 potential acidification risks, *Atmos Chem Phys*, 13, 1675-1688, 2013.

564 Pu, W. W., Quan, W. J., Ma, Z. L., Shi, X. F., Zhao, X. J., Zhang, L. N., Wang, Z. F.,
565 and Wang, W. Y.: Long-term trend of chemical composition of atmospheric
566 precipitation at a regional background station in Northern China, *Sci Total Environ*,
567 580, 1340-1350, 2017.

568 Seinfeld, J. H., and Pandis, S. N.: *Atmospheric chemistry and physics: from air
569 pollution to climate change*, Wiley, New York, 2006.

570 Shou, S. W., Zhu, Q. G., Lin, J. R., and Tang, D. S.: *The principles and methods of
571 weather science*[M], China Meteorological Press, Beijing, 76-81 pp., 2000.

572 Sportisse, B.: A review of parameterizations for modelling dry deposition and
573 scavenging of radionuclides, *Atmospheric Environment*, 41, 2683-2698,
574 10.1016/j.atmosenv.2006.11.057, 2007.

575 State Council of the People's Republic of China, Notice of the general office of the state
576 council on issuing the air pollution prevention and control action plan.
577 http://www.gov.cn/zwgk/2013-09/12/content_2486773.htm. Accessed 21 August
578 2019.

579 Sun, Y. L., Wang, Z. F., Du, W., Zhang, Q., Wang, Q. Q., Fu, P. Q., Pan, X. L., Li, J.,
580 Jayne, J., and Worsnop, D. R.: Long-term real-time measurements of aerosol
581 particle composition in Beijing, China: seasonal variations, meteorological effects,
582 and source analysis, *Atmos Chem Phys*, 15, 10149-10165, 2015.

583 Tan, J., Fu, J. S., Carmichael, G. R., Itahashi, S., Tao, Z., Huang, K., Dong, X., Yamaji,
584 K., Nagashima, T., Wang, X., Liu, Y., Lee, H. J., Lin, C. Y., Ge, B., Kajino, M.,
585 Zhu, J., Zhang, M., Liao, H., and Wang, Z.: Why do models perform differently on
586 particulate matter over East Asia? A multi-model intercomparison study for MICS-
587 Asia III, *Atmos. Chem. Phys.*, 20, 7393-7410, 10.5194/acp-20-7393-2020, 2020.

588 Tang, A. H., Zhuang, G. S., Wang, Y., Yuan, H., and Sun, Y. L.: The chemistry of
589 precipitation and its relation to aerosol in Beijing, *Atmos Environ*, 39, 3397-3406,

590 DOI 10.1016/j.atmosenv.2005.02.001, 2005.

591 Tang, J. C. H. B., Yu, X. L., Wang, S., Yao, P., Lv, B., Xu, X. B., and Ding, G.:
592 Evaluation of results of station inter-comparison with blind samples in Acid Rain
593 Monitoring Network in China, *Meteoro. Monthly*, 33, 75–83, 2007 (in English
594 abstract).

595 Tang, J., Xu, X., Ba, J., and Wang, S.: Trends of the precipitation acidity over China
596 during 1992–2006, *Chinese. Sci. Bul.*, 5, 1800–1807, doi:10.1007/s11434-009-
597 3618-1, 2010.

598 Textor, C., Schulz, M., Guibert, S., Kinne, S., Balkanski, Y., Bauer, S., Berntsen, T.,
599 Berglen, T., Boucher, O., Chin, M., Dentener, F., Diehl, T., Easter, R., Feichter, H.,
600 Fillmore, D., Ghan, S., Ginoux, P., Gong, S., Kristjansson, J. E., Krol, M., Lauer,
601 A., Lamarque, J. F., Liu, X., Montanaro, V., Myhre, G., Penner, J., Pitari, G., Reddy,
602 S., Seland, O., Stier, P., Takemura, T., and Tie, X.: Analysis and quantification of
603 the diversities of aerosol life cycles within AeroCom, *Atmos Chem Phys*, 6, 1777-
604 1813, 2006.

605 Vet, R., Artz, R. S., Carou, S., Shaw, M., Ro, C. U., Aas, W., Baker, A., Bowersox, V.
606 C., Dentener, F., Galy-Lacaux, C., Hou, A., Pienaar, J. J., Gillett, R., Forti, M. C.,
607 Gromov, S., Hara, H., Khodzher, T., Mahowald, N. M., Nickovic, S., Rao, P. S. P.,
608 and Reid, N. W.: A global assessment of precipitation chemistry and deposition of
609 sulfur, nitrogen, sea salt, base cations, organic acids, acidity and pH, and
610 phosphorus, *Atmos Environ*, 93, 3-100, 2014.

611 Wang, W. X., and Wang, T.: On acid rain formation in China, *Atmos Environ*, 30, 4091-
612 4093, 1996.

613 Wang, X., Zhang, L., and Moran, M. D.: Uncertainty assessment of current size-
614 resolved parameterizations for below-cloud particle scavenging by rain, *Atmos.
615 Chem. Phys.*, 10, 5685-5705, 10.5194/acp-10-5685-2010, 2010.

616 Wang, X., Zhang, L., and Moran, M. D.: Development of a new semi-empirical
617 parameterization for below-cloud scavenging of size-resolved aerosol particles by
618 both rain and snow, *Geosci Model Dev*, 7, 799-819, 10.5194/gmd-7-799-2014,
619 2014.

620 Wang, Y., Xue, L. I., Li, Y. A. O., Yanan, Z., and Yuepeng, P. A. N.: Variation of pH and
621 Chemical Composition of Precipitation by Multi-step Sampling in Summer of
622 Beijing 2007 (in english abstract), 30, 2715-2721, 2009.

623 Wang, Z. F., Xie, F. Y., Sakurai, T., Ueda, H., Han, Z. W., Carmichael, G. R., Streets,
624 D., Engardt, M., Holloway, T., Hayami, H., Kajino, M., Thongboonchoo, N.,
625 Bennet, C., Park, S. U., Fung, C., Chang, A., Sartelet, K., and Amann, M.: MICS-
626 Asia II: Model inter-comparison and evaluation of acid deposition, *Atmos Environ*,
627 42, 3528-3542, 2008.

628 Xu, D., Ge, B., Chen, X., Sun, Y., Cheng, N., Li, M., Pan, X., Ma, Z., Pan, Y., and Wang,
629 Z.: Multi-method determination of the below-cloud wet scavenging coefficients of
630 aerosols in Beijing, China, *Atmos. Chem. Phys.*, 19, 15569-15581, 10.5194/acp-
631 19-15569-2019, 2019.

632 Xu, D. H., Ge, B. Z., Wang, Z. F., Sun, Y. L., Chen, Y., Ji, D. S., Yang, T., Ma, Z. Q.,
633 Cheng, N. L., Hao, J. Q., and Yao, X. F.: Below-cloud wet scavenging of soluble

634 inorganic ions by rain in Beijing during the summer of 2014, Environ Pollut, 230,
635 963-973, 10.1016/j.envpol.2017.07.033, 2017.

636 Yamagata, S., Kobayashi, D., Ohta, S., Murao, N., Shiobara, M., Wada, M., Yabuki, M.,
637 Konishi, H., and Yamanouchi, T.: Properties of aerosols and their wet deposition in
638 the arctic spring during ASTAR2004 at Ny-Alesund, Svalbard, Atmos Chem Phys,
639 9, 261-270, 2009.

640 Yang, F., Tan, J., Shi, Z. B., Cai, Y., He, K., Ma, Y., Duan, F., Okuda, T., Tanaka, S., and
641 Chen, G.: Five-year record of atmospheric precipitation chemistry in urban Beijing,
642 China, Atmos Chem Phys, 12, 2025-2035, DOI 10.5194/acp-12-2025-2012, 2012.

643 Yu, Z. Y., He, L. F., Fan, G. Z., Li, Z. C., and Su, Y. L.: The basic features of the severe
644 convection at the background of cold vortex over north China (in English abstract),
645 J Trop Meteor, 27, 89-94, 2011.

646 Yuan, W. H., Sun, W., Chen, H. M., and Yu, R. C.: Topographic effects on
647 spatiotemporal variations of short-duration rainfall events in warm season of
648 central North China, J Geophys Res-Atmos, 119, 11223-11234, 2014.

649 Zhang, C., Zhang, Q., Wang, Y., and Liang, X.: Climatology of warm season cold
650 vortices in East Asia: 1979-2005, Meteorol Atmos Phys, 100, 291-301, 2008.

651 Zhang, L., Michelangeli, D. V., and Taylor, P. A.: Numerical studies of aerosol
652 scavenging by low-level, warm stratiform clouds and precipitation, Atmos Environ,
653 38, 4653-4665, <https://doi.org/10.1016/j.atmosenv.2004.05.042>, 2004.

654 Zhang, L., Wang, X., Moran, M. D., and Feng, J.: Review and uncertainty assessment
655 of size-resolved scavenging coefficient formulations for below-cloud snow
656 scavenging of atmospheric aerosols, Atmospheric Chemistry and Physics, 13,
657 10005-10025, 10.5194/acp-13-10005-2013, 2013.

658 Zhang, Q., Zheng, Y. X., Tong, D., Shao, M., Wang, S. X., Zhang, Y. H., Xu, X. D.,
659 Wang, J. N., He, H., Liu, W. Q., Ding, Y. H., Lei, Y., Li, J. H., Wang, Z. F., Zhang,
660 X. Y., Wang, Y. S., Cheng, J., Liu, Y., Shi, Q. R., Yan, L., Geng, G. N., Hong, C. P.,
661 Li, M., Liu, F., Zheng, B., Cao, J. J., Ding, A. J., Gao, J., Fu, Q. Y., Huo, J. T., Liu,
662 B. X., Liu, Z. R., Yang, F. M., He, K. B., and Hao, J. M.: Drivers of improved
663 PM2.5 air quality in China from 2013 to 2017, P Natl Acad Sci USA, 116, 24463-
664 24469, 2019.

665 Zheng, B., Tong, D., Li, M., Liu, F., Hong, C., Geng, G., Li, H., Li, X., Peng, L., Qi, J.,
666 Yan, L., Zhang, Y., Zhao, H., Zheng, Y., He, K., and Zhang, Q.: Trends in China's
667 anthropogenic emissions since 2010 as the consequence of clean air actions, Atmos.
668 Chem. Phys. Discuss., 2018, 1-27, 10.5194/acp-2018-374, 2018.

669 Zheng, Y. F., Wang L. W., and Du, J. Y.: Comparative Analysis of the Features of
670 Precipitating and Nonprecipitating Ice Clouds in the BeijingTianjin-Hebei Region
671 in Summer (in english abstract),, Climatic and Environmental Research, 25, 77-89,
672 10.3878/j.issn.1006-9585.2019.18091, 2020.

673

674

675 Table 1. Correlation of the concentrations of major ions in air in the six hours before
 676 rainfall with those in precipitation. Pearson correlation coefficients are presented for
 677 monthly volume weighted average (VWA) concentrations and for the first fraction (F1[#])
 678 in each event.

	SO₄²⁻ (n=13)	NO₃⁻ (n=14)	NH₄⁺ (n=13)	Ca²⁺ (n=9)
VWA	0.70 ^a	0.53 ^b	0.65 ^a	0.47
F1 [#]	0.76 ^a	0.62 ^a	0.77 ^a	0.85 ^a

679 Note: “a” and “b” represent significant correlations at $p<0.01$ and $p<0.05$, respectively.

680

681

682 Table 2. Exponential fitting for the concentrations of major ions in different fractions of rainfall, and the contribution of below-cloud scavenging
 683 to total deposition.

Chemical component	Exponential Fitting for 50 th percentile ^a	R ² (n=11)	Asymptote value (mg/L)	Below cloud % ^b	Average of F6#-F8# (mg/L)	Below cloud % ^c	Difference % ^d	Total wet deposition (mg/m ² /yr)
SO ₄ ²⁻	y=3.17+10.28 e ^{-0.51x}	0.85	3.18	50%	3.33	48%	<3%	3423.3
NO ₃ ⁻	y=2.32+11.03 e ^{-0.45x}	0.81	2.32	59%	2.59	54%	<6%	3046.5
NH ₄ ⁺	y=1.39+5.81 e ^{-0.28x}	0.79	1.39	65%	1.95	51%	<9%	2149.5
Ca ²⁺	y=0.67+6.81 e ^{-0.6x}	0.93	0.67	52%	0.72	48%	<6%	746.0
F ⁻	y=0.04+0.24 e ^{-0.34x}	0.91	0.04	56%	0.05	40%	<10%	49.0
Cl ⁻	y=0.27+2.2 e ^{-0.6x}	0.95	0.27	53%	0.29	50%	<5%	309.7
Na ⁺	y=0.1+1.34 e ^{-0.94x}	0.91	0.10	64%	0.10	64%	<1%	150.6
K ⁺	y=0.06+0.49 e ^{-0.47x}	0.89	0.06	64%	0.07	58%	<9%	89.8
Mg ²⁺	y=0.08+0.81 e ^{-0.4x}	0.83	0.08	61%	0.11	46%	<13%	109.2

684 ^afitting for the median of each fraction in different rainfall events; ^bbelow cloud portion calculated based on the fitting curve; ^cbelow cloud portion
 685 calculated based on the average value of fractions 6 to 8 (F6#~F8#) in rainfall events; ^ddifference in concentrations between adjacent 1 mm
 686 increments after 5 mm accumulated precipitation.

687
 688

689 **Figures and captions**

690 **Figure 1.** Concentrations of SO_4^{2-} (a), NO_3^- (b), NH_4^+ (c) and Ca^{2+} (d) in each 1-mm
691 fraction of rainfall (i.e., F1#, F2#, ...) over different rainfall events in the observation
692 periods. The red line shows an exponential fitting using the 50th percentile of the data
693 and the red shading indicates the range between the 25th and 75th percentiles.

694 **Figure 2.** Time series of annual volume weighted average (VWA) concentration of the
695 four major components NH_4^+ (a), Ca^{2+} (b), SO_4^{2-} (c) and NO_3^- (d) in precipitation in
696 Beijing.

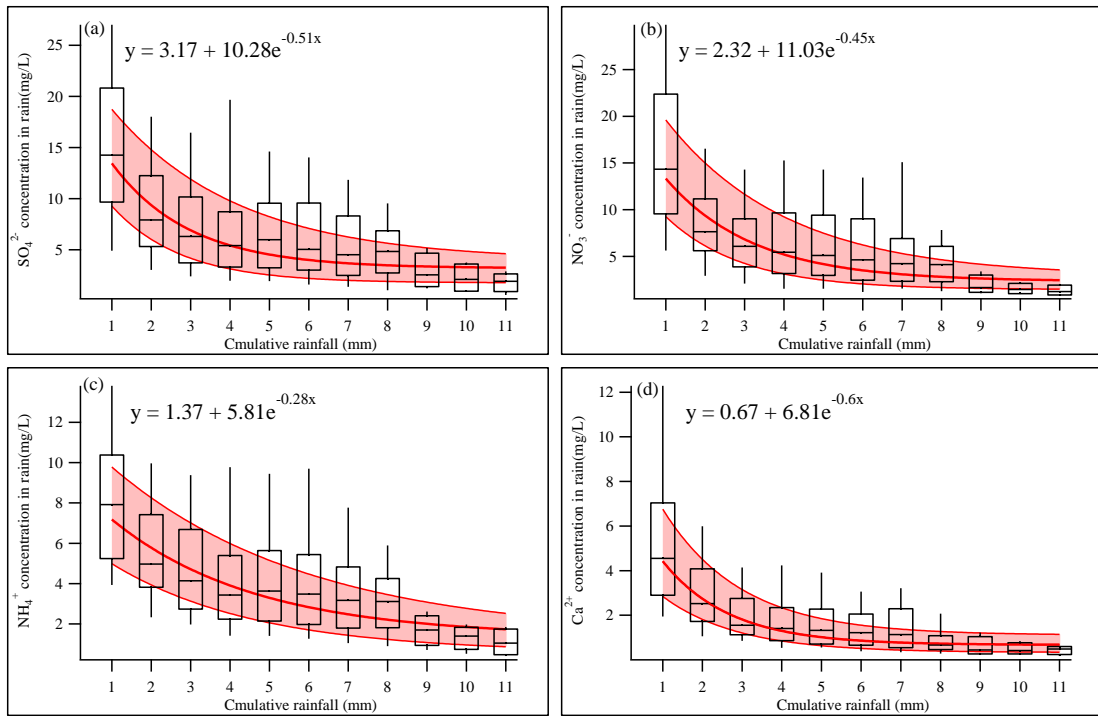
697 **Figure 3.** Annual changes in emission and concentration of SO_2 and NO_x in Beijing,
698 data is collected from the yearly book of "*Environmental Bulletin in Beijing*" from 1994
699 to 2017.

700 **Figure 4.** Relationships between the concentration of NO_3^- (a), SO_4^{2-} (b), NH_4^+ (c) and
701 Ca^{2+} (d) in precipitation and in air in the 6 h before each precipitation event. The red
702 square and blue triangle represented the relationships between the concentration of ions
703 in air with that in F1# and in VWA, respectively.

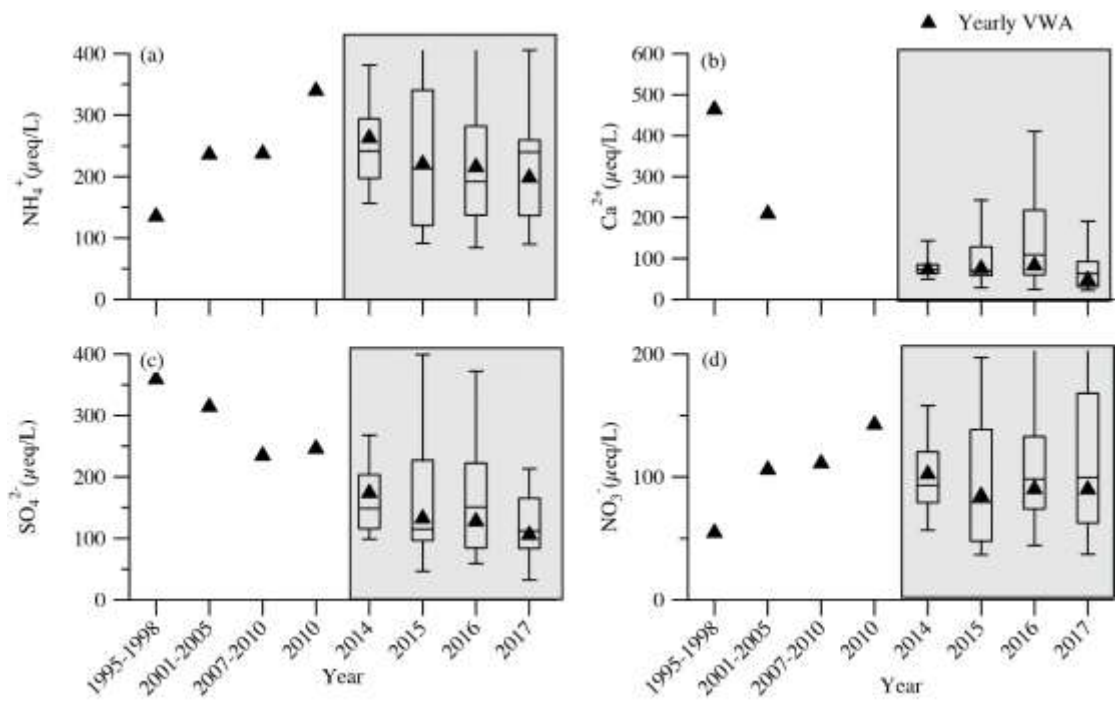
704 **Figure 5.** The annual volume weighted average below-cloud and in-cloud portion of
705 SO_4^{2-} (a), Ca^{2+} (b), NO_3^- (c), and NH_4^+ (d) during 2014-2017. The ratio of annual
706 median below-cloud contribution for each component is represented as the black line
707 in each panel. The mark #M and #A in the ratio of below-cloud represent the estimation
708 based on the median value and average value of in-cloud concentration in each year,
709 while the first quartile and the third quartiles are also included in the figure.

710 **Figure 6.** Contribution of below-cloud scavenging during rainfall events associated
711 with different synoptic conditions.

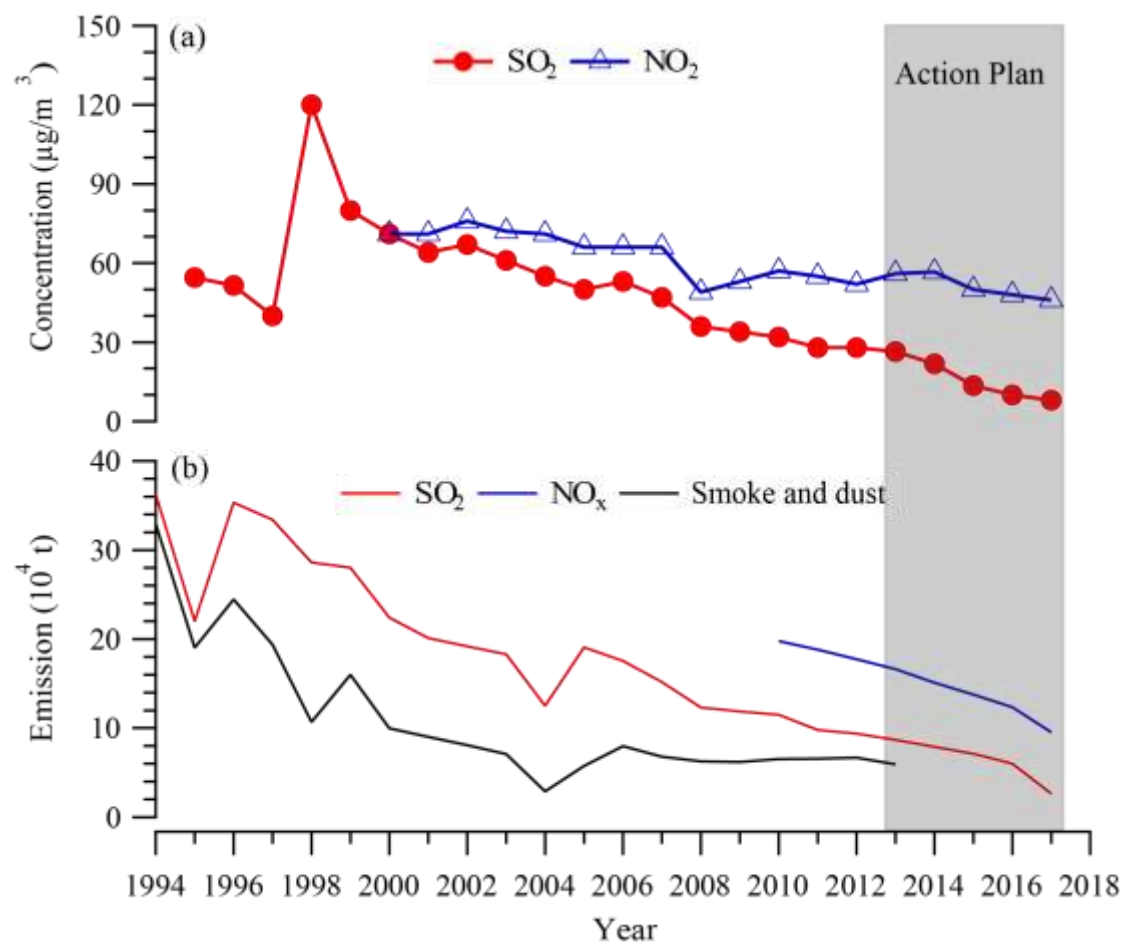
712 **Figure 7.** Contribution of below-cloud scavenging in events with different rainfall
713 volume and precipitation intensity



718 Figure 1. Concentrations of SO_4^{2-} (a), NO_3^- (b), NH_4^+ (c) and Ca^{2+} (d) in each 1-mm
 719 fraction of rainfall (i.e., F1#, F2#, ...) over different rainfall events in the observation
 720 periods. The red line shows an exponential fitting using the 50th percentile of the data
 721 and the red shading indicates the range between the 25th and 75th percentiles.



726 Figure 2. Time series of annual volume weighted average (VWA) concentration of the
 727 four major components NH_4^+ (a), Ca^{2+} (b), SO_4^{2-} (c) and NO_3^- (d) in precipitation in
 728 Beijing.



731 Figure 3. Annual changes in emission and concentration of SO_2 and NO_x in Beijing,
 732 data is collected from the yearly book of "Environmental Bulletin in Beijing" from
 733 1994 to 2017.

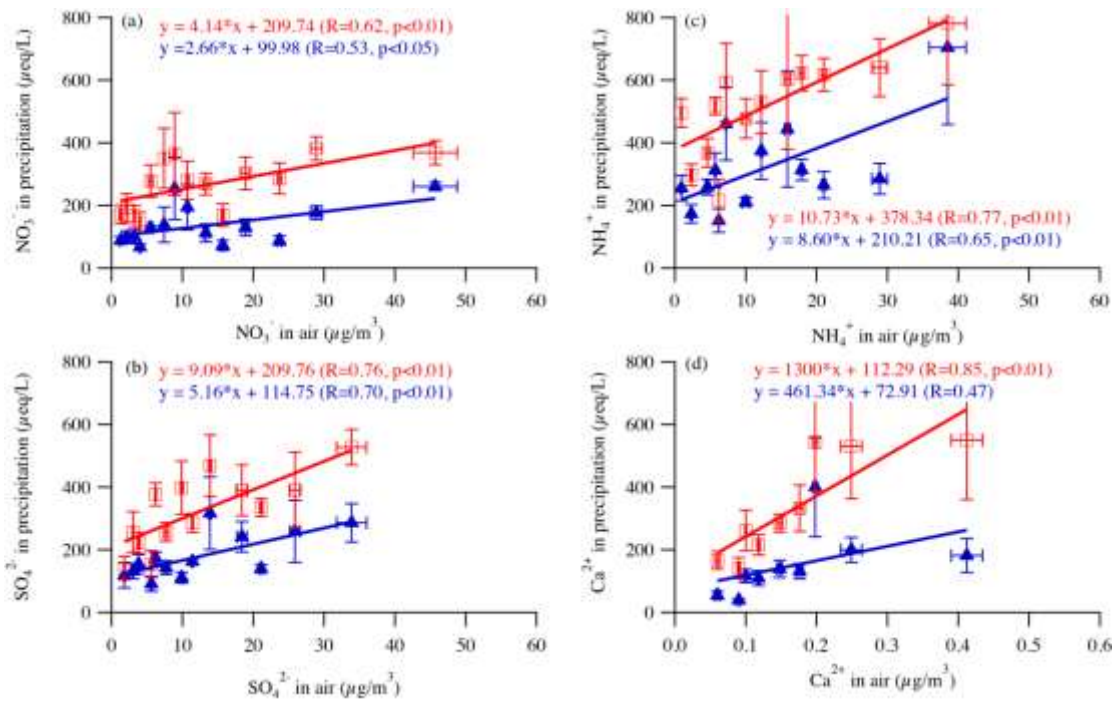
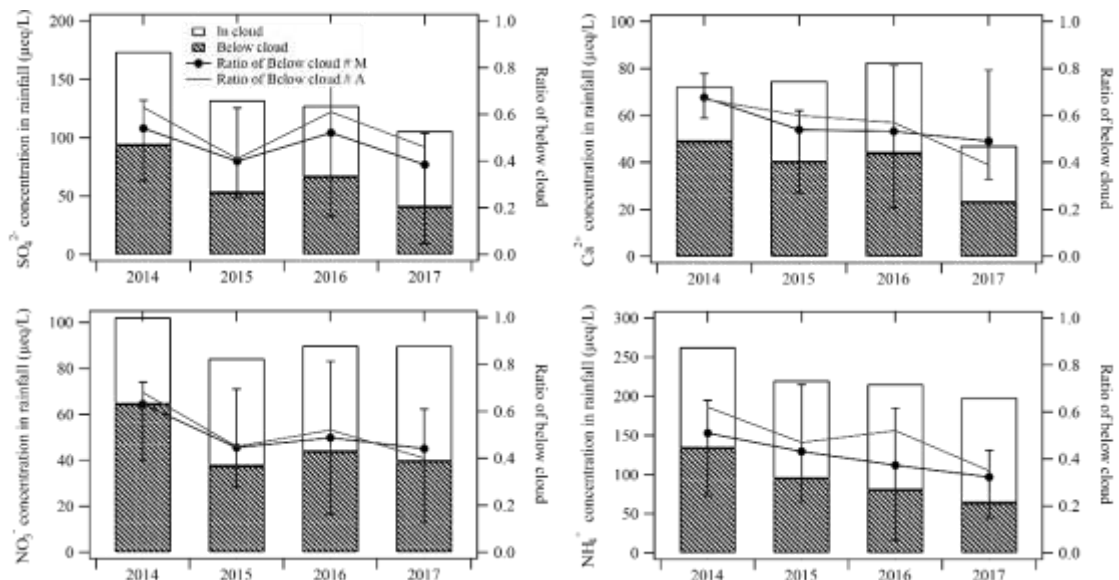
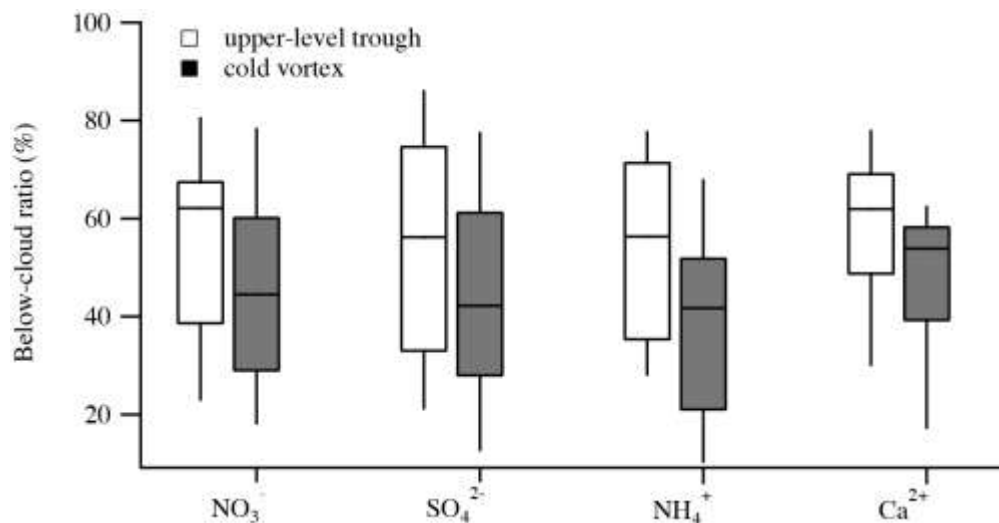


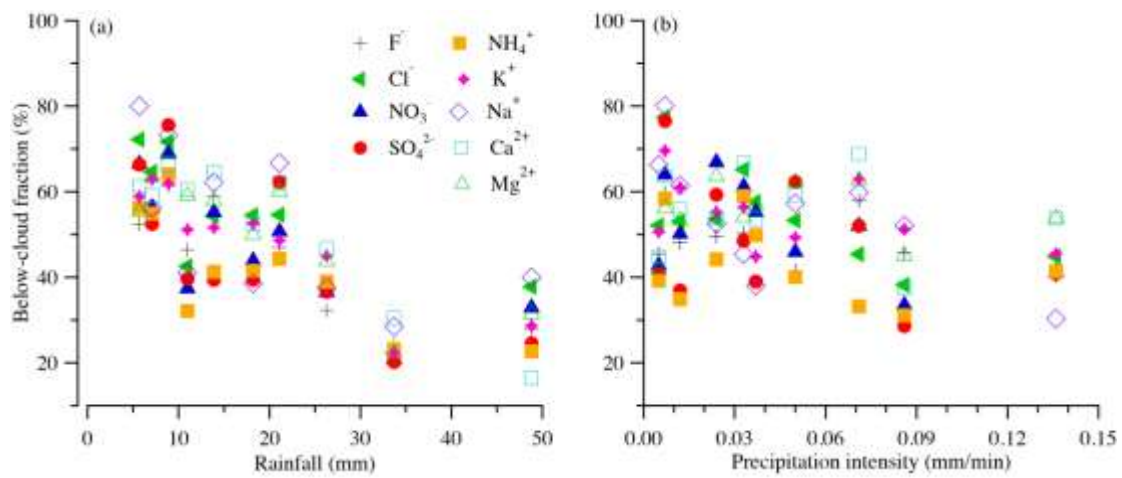
Figure 4. Relationships between the concentration of NO_3^- (a), SO_4^{2-} (b), NH_4^+ (c) and Ca^{2+} (d) in precipitation and in air in the 6 h before each precipitation event. The red square and blue triangle represented the relationships between the concentration of ions in air with that in F1# and in VWA, respectively.



742 **Figure 5.** The annual volume weighted average below-cloud and in-cloud portion of
743 SO_4^{2-} (a), Ca^{2+} (b), NO_3^- (c), and NH_4^+ (d) during 2014-2017. The ratio of annual
744 median below-cloud contribution for each component is represented as the black line
745 in each panel. [The mark #M and #A in the ratio of below-cloud represent the estimation
746 based on the median value and average value of in-cloud concentration in each year,
747 while the first quartile and the third quartiles are also included in the figure.](#)



751 Figure 6. Contribution of below-cloud scavenging during rainfall events associated
 752 with different synoptic conditions.



756 Figure 7. Contribution of below-cloud scavenging in events with different rainfall
 757 volume and precipitation intensity.